Human Reproduction, Vol.25, No.1 pp. 42–51, 2010
Advanced Access publication on October 14, 2009 doi:10.1093/humrep/dep359

human reproduction

ORIGINAL ARTICLE *Andrology*

Characterization of a novel cell-surface protein expressed on human sperm

Ruey-Bing Yang[1,2,†], Heng-Kien Au[3,4,†], Chii-Ruey Tzeng[3,4], Ming-Tzu Tsai[1], Ping Wu[5,6], Yu-Chih Wu[5,6,7], Thai-Yen Ling[8], and Yen-Hua Huang[4,5,6,9]

[1]Institute of Biomedical Sciences, Academia Sinica, Taipei, Taiwan [2]Institute of Pharmacology, School of Medicine, National Yang-Ming University, Taipei, Taiwan [3]Department of Obstetrics and Gynecology, School of Medicine, Taipei, Taiwan [4]Center for Reproductive Medicine, Taipei Medical University and the Hospital, Taipei, Taiwan [5]Department of Biochemistry, College of Medicine, Taipei Medical University, Taipei, Taiwan [6]Graduate Institute of Medical Sciences, College of Medicine, Taipei Medical University, Taipei, Taiwan [7]Graduate Institute of Life Sciences, National Defense Medical Center, Taipei, Taiwan [8]Institute of Pharmacology, National Taiwan University, Taipei, Taiwan

[9]Correspondence address. Tel: +886-2-27361661-3150; Fax: +886-2-2735-6689; E-mail:rita1204@tmu.edu.tw

BACKGROUND: Precise sperm–oocyte interaction is a critical event for successful fertilization. However, the identity of molecules involved in this process in humans remains largely unknown. This report describes the identification and characterization of a novel cell-surface protein and its potential role in human sperm–oocyte interaction.

METHODS AND RESULTS: We previously identified an orphan guanylyl cyclase receptor (mouse GC-G) highly enriched in mouse testis and involved in sperm activation. By using a comparative genomic approach, we found the homologue gene in human (hGC-G) composed of 21 exons, spanning a minimum of 48 kb on chromosome 10q25. Real-time RT–PCR analysis revealed hGC-G mRNA selectively expressed in testis but with low or no expression in all other tissues examined. Compared with mGC-G, the hGC-G transcript contains three 1-bp deletions and two in-frame termination codons, which results in a short putative receptor-like polypeptide. Western blot analysis with an anti-hGC-G-specific antibody confirmed the protein expression of hGC-G in human sperm lysate. Flow cytometry and confocal immunofluorescence analysis demonstrated the localization of hGC-G protein on the acrosome cap and equatorial segment of mature human sperm. In addition, an integrin-binding Arg-Gly-Asp (RGD) motif was found in the extracellular domain of hGC-G. Pre-incubation of the hGC-G RGD peptide with zona pellucida-free oocytes greatly decreased the binding of human sperm to hamster oocytes, which suggests a role for hGC-G role in sperm–oocyte interaction.

CONCLUSIONS: hGC-G is a novel surface protein on human sperm and potentially mediates sperm–oocyte interaction through its RGD-containing motif.

Key words: cell-surface protein / human sperm / RGD motif / integrin / gamete interaction

Introduction

In sexually reproductive species, the precise recognition between sperm and oocyte is the most important process in successful fertilization. Current evidence suggests that several molecules on the sperm cell surface interact with the oocyte to complete the sperm–oocyte interaction; examples are CD46 (membrane cofactor protein) (Anderson *et al*., 1993; Inoue *et al*., 2003), mouse sperm lysozyme-like protein (mSLLP1) (Herrero *et al*., 2005), epididymal-derived cysteine-rich secretory protein 1 (CRISP-1) (Cuasnicu *et al*., 1984; Da Ros *et al*., 2008), ERp57 (Pdi3a) (Ellerman *et al*., 2006), Izumo (Inoue *et al*., 2005), and the three ADAMs (a disintegrin and metalloprotease domain) proteins. The ADAMs include fertilin α (ADAM1), fertilin β (ADAM2) and cyritestin (ADAM3), which are expressed on the sperm cell surface to provide an Arg-Gly-Asp (RGD) motif for interaction with integrins on the oocyte (Evans *et al*., 1995; Yuan *et al*., 1997; Primakoff and Myles, 2000). Integrins are a family of cell adhesion molecules that mediate cell–cell and cell–extracellular matrix interaction. They exist as heterodimers, for which at least 18α and 8β subunits have been identified, and different subunit combinations give rise to 24 different integrins (Evans, 2002). On the oocyte surface, the integrin of α6β1 has been implicated in both the ADAM2 and ADAM3 interaction in sperm (Bigler *et al*., 2000; Takahashi *et al*., 2001). Although the possible mechanisms of

†These authors contributed equally to this work.

sperm–oocyte interaction have been reported for many species, gene-knockout of several of these molecules has not affected fertility or sperm–oocyte interaction (Cho *et al*., 1998; Nishimura *et al*., 2001; Inoue *et al*., 2003; Da Ros *et al*., 2008). Furthermore, the recognition molecules on the human sperm surface are still not completely known.

Intracellular cyclic GMP (cGMP) acts a second messenger in the regulation of a broad spectrum of tissue functions, such as intestinal secretion, smooth-muscle relaxation, retinal phototransduction, platelet activation and sperm activation (Vaandrager and De Jonge, 1994; Warner *et al*., 1994; Schlossmann *et al*., 2003; Huang *et al*., 2006; Kuhn, 2009). In mammals, the cGMP-generating enzymes [guanylyl cyclases (GCs)] are divided into two major classes: those that contain no apparent transmembrane segment (the soluble form) and those that contain one transmembrane segment (the receptor form) (Tamura *et al*., 2001). To date, seven receptor GCs have been identified in mammals, termed GC-A to GC-G in order of their discovery (Chinkers *et al*., 1989; Lowe, *et al*., 1989, 1995; Schulz *et al*., 1989, 1990, 1998; Koller *et al*., 1991; Shyjan *et al*., 1992; Fulle *et al*., 1995; Matsuoka *et al*., 1995; Kuhn *et al*., 2004; Kuhn, 2009). These proteins form a family of type I cell-surface receptors and share a common domain organization: an extracellular ligand-binding domain, a single membrane-spanning segment, and a cytoplasmic region that can be subdivided into a protein kinase-like domain and a carboxyl-terminal cyclase catalytic domain (Garbers, 1999; Kuhn, 2009). The peptide ligands have been identified for only four of the receptor GCs (GC-A, -B, -C and -D), and the other three membrane GCs remain known as orphan receptors (Kuhn, 2009).

The mouse GC-G (mGC-G), the most recent member of the receptor GC family, was identified from the mouse testis (Kuhn *et al*., 2004). mGC-G is highly and selectively expressed in mouse testis. All ligands known to activate other receptor GCs have failed to stimulate its enzymatic activity (Kuhn *et al*., 2004). However, when overexpressed in human embryonic kidney (HEK)-293T cells, the recombinant mGC-G exhibits marked cGMP-generating GC activity. In addition, use of a specific neutralizing antibody demonstrated mGC-G to play an important role in regulation of sperm motility and capacitation (Huang *et al*., 2006). Furthermore, under pathophysiological conditions, mGC-G has been found to contribute to tubular damage and renal failure through apoptosis and inflammation (Lin *et al*., 2008). However, the biological function and physiological regulation of GC-G remains elusive.

In this study, to further explore the possible biological role of GC-G in humans, we identified and characterized the apparent human homologue of GC-G (hGC-G) by the comparative genomic approach. The hGC-G gene, *GUCY2GP*, resides on human chromosome 10q25.2, spans a minimum of ~48 kb, has at least 21 exons, and contains an RGD-motif at the extracellular domain (ECD). This gene is highly expressed in human testis but has a series of differently processed transcripts that contain some insertions, deletions or in-frame termination codons. However, the hGC-G still translates into a receptor-like transmembrane protein and locates on the plasma membrane overlying the acrosome cap and equatorial segment of the sperm head. We further verified by hGC-G RGD and/or hGC-G RGE peptide competition assay that the RGD motif of the hGC-G ECD produces a functional interaction between sperm and oocyte during fertilization. Our results suggest that the hGC-G is a receptor-like cell-surface protein that participates in sperm–oocyte binding through its RGD-containing motif.

Materials and Methods

Reagents and cells

Two independent panels of human tissue cDNAs were obtained from BD-Clontech or OriGene Technologies (Rockville, MD, USA). High-fidelity PfuTurbo polymerase was from Stratagene (La Jolla, CA, USA). The PCR products were cloned into pGEM-T Easy plasmid vector (Promega). Human testis tissue lysate was purchased from BioChain Institute, Inc. (Hayward, CA, USA). Human sperm samples were from the Department of Obstetrics and Gynecology, Center for Reproductive Medicine, Taipei Medical University and Hospital. This study was approved by the institutional ethical and review board of Taipei Medical University for the protection of human subjects.

Database searches and sequence analysis of hGC-G

The coding sequence of mGC-G was first used as a template to search against the human genome database, utilizing the Blat program available from http://www.genome.ucsc.edu. The initial set of BLAST hits was mapped on the human chromosome 10q25.2 region with use of the genome-view option. The sequence of a BAC clone (GenBank accession no. AL157786) containing the hGC-G gene was then downloaded and compared in a pair-wise fashion with the sequence of each individual exon (21 exons) of mGC-G to refine the exon–intron boundaries in the hGC-G gene. The resulting exons corresponding to the putative coding sequence of hGC-G were joined, translated into a protein sequence and analyzed by use of the LASERGENE suite of programs (DNASTAR, Madison, WI, USA).

Tissue distribution of the hGC-G mRNA

Quantitative real-time RT–PCR (TaqMan) analyses involved use of the PRISM 7700 Sequence Detection System (Applied Biosystems, Foster City, CA, USA) with a panel of human fetal and adult tissue cDNAs (BD Clontech, Palo Alto, CA, USA). Normalization was to the level of glyceraldehyde-3-phosphate dehydrogenase (GAPDH) mRNA as a control. Probes were designed by use of PrimerExpress software (PE Applied Biosystems) on the basis of the predicted sequence of the hGC-G gene. The gene-specific TaqMan probe was labeled with FAM (6-carboxyfluorescein) at the 5′ end and BHQ1 (black hole quencher) linked at the 3′ end as quenchers (Biosource International, Camarillo, CA, USA). The following primers and fluorescent probes were used: for hGC-G, 5′ primer: tgc cgc agt agg gct tta tc; hGC-G 3′ primer: gct tcc taa ccc agg ctt ctg; hGC-G probe: 5′-FAM-cca tgt ggc cat ccg tta cgt tgg-BHQ1; for GAPDH, 5′ primer: tga agg tcg gag tca acg g; GAPDH 3′ primer: aga gtt aaa agc agc cct ggt g, and GAPDH probe: 5′-FAM-ttt ggt cgt att ggg cgc ctg g-BHQ1. To confirm the tissue expression of hGC-G, PCR reactions involved use of a pair of hGC-G-specific oligonucleotides (Primer 1; 5′-aaa gac atc tgg tgg caa atc-3′ and Primer 2; 5′-ttt ggt tga tga ttt cat ccg-3′, Fig. 1) from an independent panel of human cDNAs (OriGene Technologies). The resulting PCR products were separated on an agarose gel, transferred onto a nylon membrane and hybridized by use of a [^{32}P]-labeled cDNA probe. Autoradiography was performed at 25°C for 15 min.

The tissue distribution of hGC-G transcripts was also analyzed by Southern blot analysis. A fragment of the hGC-G cDNA from a panel of human fetal and adult cDNAs was amplified by PCR with use of specific

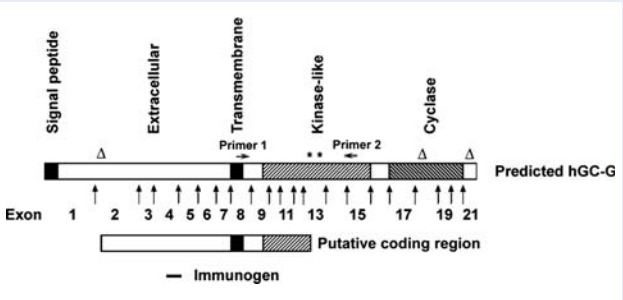

Figure 1 The domain organization of the predicted hGC-G.

The putative coding sequence of hGC-G was extracted from the human genome database as described under 'Materials and Methods'. The extracellular domain, transmembrane domains and the intracellular kinase-like and cyclase domains of hGC-G are described in Supplementary Figures. The positions of three 1-bp deletions (Δ) and two in-frame termination codons (*) are marked. The positions of the putative intron–exon boundary based on the genomic organization of the mGC-G gene are indicated by arrows. The longest putative open reading frame is depicted. The horizontal bar marks the location of one immunogene used to create the anti-hGC-G-specific polyclonal antibody.

primers (Primers 1 and 2), then were transferred onto a nylon membrane and hybridized with the hGC-G-specific probe.

Preparation of rabbit polyclonal antisera to hGC-G

One peptide, NH_2-GTPRRSPFRSTISWEEQVSPC-COOH (derived from the ECD of hGC-G), was used as an antigen to immunize New Zealand White rabbits. The rabbits were given an initial subcutaneous injection of 0.5 mg of the recombinant peptide protein emulsified in 1 ml of Freund's complete adjuvant. Subsequently, rabbits received 2–3 booster injections of 0.25 mg recombinant protein with Freund's incomplete adjuvant. Antisera were recovered from blood obtained by terminal exsanguination and further subjected to Protein-A column processing for partial purification.

Preparation of human sperm and human sperm lysate

The human sperm preparation was as described previously (Brandelli *et al.*, 1994). In brief, human semen was liquefied at 37°C for 60 min, and then separated by 30–60% Percoll BWW medium (Biggers *et al.*, 1971). The sperm fraction with good motility was collected after three washes with the same medium to remove semen protein and fatty acid, and then resuspended in defined medium for further use.

The human sperm lysate was prepared as described (Visconti *et al.*, 1995). In brief, the Percoll-separated human sperm was washed with phosphate-buffered saline (PBS) and then completely lysed in 2× Laemmli sample buffer with β-mercaptoethanol and boiled for 5 min. After centrifugation at 5000*g* for 3 min, the supernatant was collected and boiled in the presence of 5% β-mercaptoethanol for 5 min, then subjected to SDS-PAGE as described below.

Preparation of recombinant hGC-G or mGC-G protein

The FLAG-tagged recombinant hGC-G or mGC-G proteins were produced by HEK-293T cells after transient transfection of expression plasmid coding for FLAG.hGC-G or FLAG.mGC-G as described (Kuhn *et al.*, 2004). The FLAG epitope tag was added at the amino terminus for easy detection of recombinant proteins by western blot analysis or fluorescence-activated cell sorting (FACS) analysis with anti-FLAG antibody.

Western blot analysis of hGC-G

Percoll-separated human sperm cell lysate (20 μg), recombinant protein of FLAG.hGC-G and FLAG.mGC-G, or human testis tissue lysate (20 μg) was boiled in Laemmli sample buffer, separated by SDS-PAGE, and transferred to polyvinylidene difluoride membranes. The membranes were blocked with PBS (pH 7.5) containing 5% skim milk and 0.05% (v/v) Tween-20 and then incubated with four different polyclonal antisera: anti-hGC-G, anti-FLAG, preimmune serum, or control rabbit IgG (10 μg/ml each). After two washes, the blots were incubated with horseradish peroxidase (HRP)-conjugated goat anti-rabbit IgG (1: 2000) (Jackson ImmunoResearch, West Grove, PA, USA) for 1 h. After membranes were washed, the immunoreactive bands were visualized with use of an enhanced chemiluminescence system (ECL; Amersham).

Capacitation and acrosome reaction of human sperm

The Percoll-separated human sperm samples were prepared and resuspended in the Ca^{2+}-free BWW medium supplemented with 0.3% bovine serum albumin (BSA) at 2×10^6 cells/ml. For sperm capacitation, human sperm samples in medium were incubated at 37°C and 5% CO_2 for 60–180 min. For sperm acrosome reaction, the capacitated human sperm samples were treated with A23187 (5 μM, Sigma) at 37°C and 5% CO_2 for 15 min.

Detection of protein tyrosine phosphorylation

Percoll-purified human sperm samples (5×10^6 cells/ml) in Ca^{2+}-free BWW medium were pre-incubated with anti-hGC-G IgG (20 μM), control IgG (20 μM) or control medium at 37°C for 15 min, then equal volumes of BSA (0.6%) or control medium with or without anti-hGC-G IgG or control IgG (both 20 μM) were added into the specified culture medium. In the BSA group, the final concentration of BSA was 0.3%. Concentrations of the anti-hGC-G IgG or control IgG remained unchanged. The sperm samples were further incubated at 37°C in 5% CO_2 for an additional 3 h. After incubation, the human sperm lysate was collected and underwent 10% SDS-PAGE, and then was transferred to a PVDF membrane for western blot analysis as described previously (Huang *et al.*, 2006) with the primary monoclonal anti-phosphotyrosine IgG (clone 4G10, UBI) (1 μg/ml) and secondary HRP-conjugated anti-mouse IgG antibodies (1: 2000). The enzyme activity of HRP was detected by the ECL system according to the manufacturer's instructions.

Sperm–oocyte binding

To collect oocytes, mature hamster female mice underwent ovulation induction with an injection (intraperitoneal) of pregnant mare serum gonadotrophin (25 IU; Syntex), then were given an intraperitoneal injection of human chorionic gonadotrophin (hCG; 25 IU; Sigma) after 48 h. The oocytes were collected from the oviducts of superovulated animals 12–13 h after hCG administration. Cumulus cells were removed by incubating the oocyte–cumulus complexes for 3 min in 0.3 mg/ml hyaluronidase (type IV; Sigma). The zona pellucida layers were then dissolved by treating the oocytes with acid Tyrode solution (pH 2.5) for 10–20 s (Nicolson *et al.*, 1975).

For competition assay of hGC-G RGD or hGC-G RGE peptide on sperm–oocyte binding, the zona pellucida-free oocytes were pre-incubated with medium containing hGC-G RGD or hGC-G RGE (0.5 mM) at 37°C for 2 h. After a brief wash to remove the free hGC-G peptide, the zona pellucida-free oocytes were co-incubated with capacitated sperm (final concentration 10^6 sperm/ml) for 0–60 min at 37°C under 5% CO_2. The sperm cells adhering to each zona pellucida-free oocyte were counted and analyzed.

Histological and cytological studies

For immunocytochemical staining, freshly prepared human sperm were fixed in 3.7% paraformaldehyde/PBS at room temperature for 30 min in Eppendorf tubes. After fixation, the cells were rinsed with PBS twice, and then treated with PBS containing 0.1% Triton-X 100 (PBST) at room temperature for 10 min and blocked with BSA (5 mg/ml) in PBST for 1 h at room temperature. The cells were then incubated at 4°C overnight with the primary anti-hGC-G IgG antibody (10 μg/ml) with gentle shaking. After three washes with PBS, the cells were incubated with the secondary Cy3-conjugated anti-rabbit IgG antibody (1:1000) at room temperature for 1 h. After washes, the sperm cells were counterstained with FITC-PSA (20 μg/ml, Sigma) for acrosome staining and DAPI for nucleus (Sigma). The sperm samples were then smeared on slides, covered with anti-fading reagent (Vector Laboratories), and visualized by epifluorescence (Olympus) and confocal fluorescence microscopy (Leica).

Mature sperm were also collected and stained with anti-hGC-G IgG (10 μg/ml) or control rabbit IgG, then FITC-conjugated anti-rabbit IgG secondary antibody, and were analyzed by FACS analysis.

Statistical analysis

All experiments were repeated at least three times with three different pooled sperm samples. All statistical tests involved use of Graph Pad Instat 3.00 (GraphPad Software, La Jolla, CA, USA). To compare the cell adhesion ability of hGC-G RGD-HEK-293 or hGC-G RGE-HEK-293 cells on a fibronectin (FN)-coated cell plate, we determined the cell adhesion percentage under various experimental conditions and then compared each other by one-way ANOVA, followed by the Tukey–Kramer multiple comparison test. To compare the binding ability of hGC-G RGD- or hGC-G RGE-pretreated sperm cells on zona pellucida-free oocytes, the sperm number on each oocyte was counted and compared by unpaired *t* test. The data are expressed as means ± SD, and $P < 0.05$ was considered statistically significant.

Results

In silico identification and sequence analysis of hGC-G

The nucleotide sequence of mGC-G (GenBank accession no. AY395631) derived from our previous report (Kuhn *et al.*, 2004) was used for a homology search in the human genome database (www.genome.ucsc.edu). The hGC-G gene, *GUCY2GP*, is contained in a BAC clone (GenBank accession no. AL157786) localized to chromosome 10q25.2 and is syntenic to mouse chromosome 19.D2, where the mGC-G gene resides. The gene structure and exon–intron boundaries appear to be well conserved between mGC-G and hGC-G genes, and the nucleotide sequences of the predicted mGC-G and hGC-G genes showed an overall 80% identity in coding region.

Despite a high degree of sequence identity with mGC-G, hGC-G had three 1-bp deletions and two in-frame termination codons as compared with the mouse orthologue. The first 1-bp deletion (Deletion I) is located within the ECD (Supplementary Fig. S1), and the other two (Deletions II and III) reside towards the carboxyl-terminal end of the cyclase catalytic domain (Supplementary Fig. S2). In addition, two in-frame termination codons (Stop I and II) are present within the kinase-like domain (Supplementary Fig. S2). Thus, *GUCY2GP* spans a minimum of ~48 kb and contains at least 21 exons (Fig. 1). Multiple alignment analysis comparing the putative hGC-G protein sequence with that of rat and mGC-G showed an overall 65% sequence similarity (Supplementary Fig. S3). Four cysteine residues within the ECD of GC-G are conserved among these orthologues. These cysteine residues are also invariant in other receptor GCs (Thompson and Garbers, 1995) and play an important role in maintaining the proper disulfide bonding and the ligand-binding function of receptor GCs (McNicoll *et al.*, 1996; van den Akker *et al.*, 2000).

Tissue-specific expression of hGC-G

We first used a sensitive PCR-based approach to determine the tissue distribution of hGC-G. The hGC-G-specific oligonucleotide primers and probes were designed on the basis of gene prediction to study the tissue expression profile by quantitative real-time RT–PCR (TaqMan) analysis. Among human fetal and adult tissues, hGC-G mRNA was highly expressed in the testis, and then showed a lower expression in placenta but virtually no expression in all other tissues examined (Fig. 2A). Similar results were obtained from an independent panel of tissue cDNAs by a combination of RT–PCR then Southern blot analysis (Fig. 2B). Together, these results clearly demonstrate that, like mGC-G, hGC-G is a testis-enriched gene (Kuhn *et al.*, 2004).

Expression and localization of hGC-G in sperm

To investigate whether the putative hGC-G is indeed expressed at the protein level, we generated an anti-hGC-G-specific polyclonal antibody. As shown in Fig. 3A, the antiserum could specifically detect the recombinant hGC-G protein (FLAG-tagged hGC-G) but not the FLAG-tagged mGC-G receptor in HEK-293T cells. Preimmune serum served as a negative control. The cell-surface expression of recombinant hGC-G on HEK-293T cells was further confirmed by flow cytometry (Fig. 3B).

We then performed western blot analysis to examine the protein expression of hGC-G in human sperm and testis. The human sperm was pre-separated by Percoll gradient to remove semen protein and fatty acid. As shown in Fig. 4A, as compared with the rabbit IgG control, anti-hGC-G IgG detected several specific immunoreactive bands from human sperm extracts (30–50 kDa, Cleaved). In addition, the molecular identity of hGC-G in the testis was further examined. Figure 4A showed that the anti-hGC-G IgG recognized a testis-specific protein with an apparent molecular mass of 70 kDa (asterisk), which supports the existence of an unprocessed hGC-G precursor in testis. Further immunocytochemical staining combined with flow cytometry revealed its characteristics in cell surface expression (Fig. 4B). Further, in conjunction with epifluorescence and confocal image

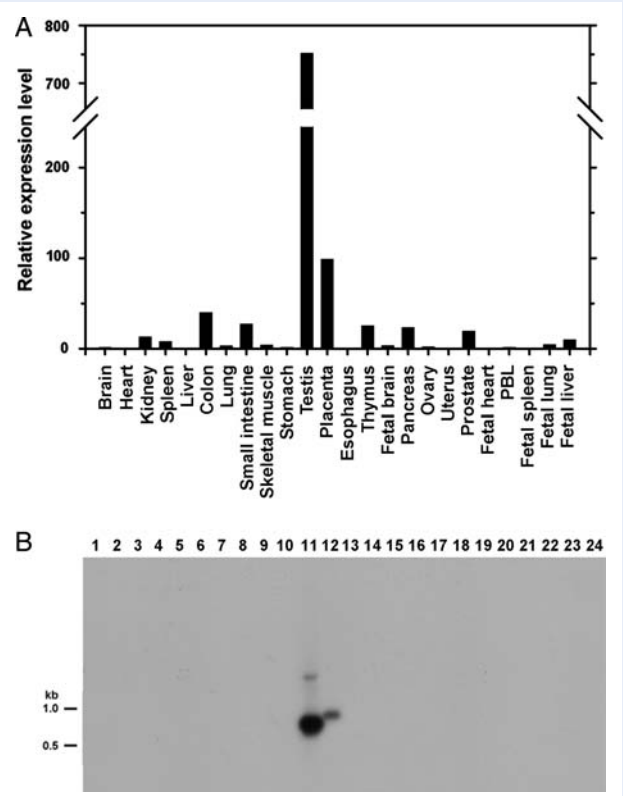

Figure 2 Testis-enriched expression of hGC-G.

(**A**) Quantitative real-time RT–PCR (TaqMan) analysis of the hGC-G mRNA expression profile. A panel of human fetal and adult tissue cDNAs was used for quantitative RT–PCR analysis with hGC-G-specific oligonucleotide pairs and probes. Expression levels were normalized to that of GAPDH. PBL, peripheral blood leukocytes. (**B**) Tissue distribution of hGC-G transcripts by RT–PCR and Southern blot analysis. A fragment of the hGC-G cDNA from a panel of human fetal and adult cDNAs was amplified by PCR with use of specific primers (Primers 1 and 2, Fig. 1), then were transferred onto a nylon membrane and hybridized with a hGC-G-specific probe. cDNA templates used were (1) brain, (2) heart, (3) kidney, (4) spleen, (5) liver, (6) colon, (7) lung, (8) small intestine, (9) muscle, (10) stomach, (11) testis, (12) placenta, (13) salivary, (14) thyroid, (15) adrenal gland, (16) pancreas, (17) ovary, (18) uterus, (19) prostate, (20) skin, (21) peripheral blood leukocytes, (22) bone marrow, (23) fetal brain and (24) fetal liver. Note that the apparent size difference of GC-G transcripts between testis and placenta may represent the differential splice variants expressed in these tissues.

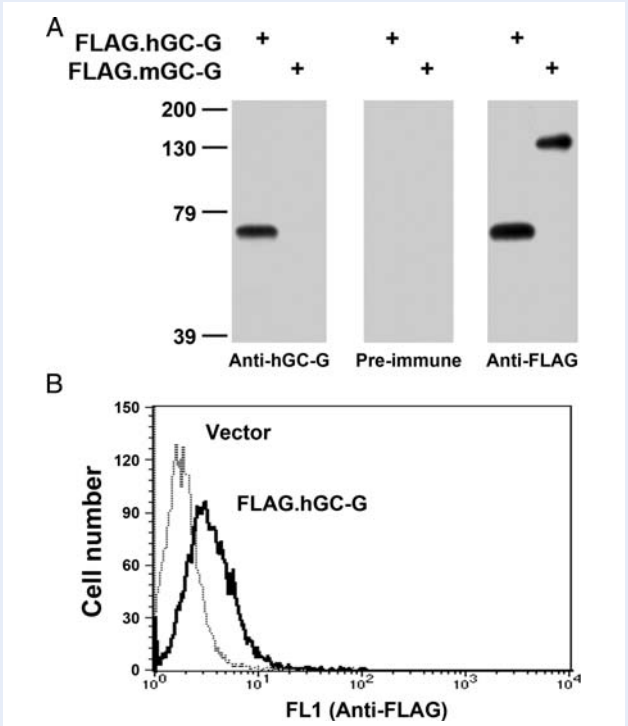

Figure 3 Expression of recombinant hGC-G protein on HEK-293T cells.

(**A**) Specificity of anti-hGC-G antibody. Anti-hGC-G polyclonal antiserum was generated in rabbits immunized with the peptide immunogen derived from the extracellular domain of hGC-G and purified by a protein A-affinity column as described in 'Materials and Methods'. The anti-hGC-G antibody could specifically recognize the recombinant FLAG-tagged hGC-G (FLAG.hGC-G) protein expressed in HEK-293T cells but not the FLAG-tagged mGC-G (upper panel). As a control, protein expression of the FLAG-tagged GC receptors was confirmed by anti-FLAG antibody. Molecular masses are indicated in kDa. (**B**) Cell-surface expression of recombinant hGC-G by flow cytometry. HEK-293T cells transiently transfected with the empty vector (Vector) or the expression plasmid encoding FLAG.hGC-G protein were stained with anti-FLAG (10 μg/ml), then an FITC-conjugated anti-mouse IgG secondary antibody, and then analyzed by fluorescence-activated cell sorting (FACS) analysis.

analysis, hGC-G was shown to be located at the tail, acrosomal cap and equatorial segment (Fig. 4C and D).

Effect of hGC-G on sperm capacitation

Because hGC-G located both at the tail and head of human sperm, we determined the role of hGC-G in sperm activation and/or fertilization. Because of a lack of known ligand or specific inhibitor for hGC-G, we tested the function of hGC-G in sperm activation by using the 'BSA activation assay model' as we reported previously (Huang *et al.*, 2006). The protein tyrosine phosphorylation is known to be molecular evidence for sperm capacitation (Carrera *et al.*, 1996, Zarelli *et al.*, 2009). Therefore, we used the anti-hGC-G-specific IgG antibody raised against a peptide immunogen within the ECD as a neutralizing reagent and detected the protein tyrosine phosphorylation level of human sperm under BSA (0.3%) treatment in the presence of the anti-hGC-G IgG or the control rabbit IgG. Consistent with a previous report, the human sperm showed a Ca^{2+}-dependent suppression of protein tyrosine phosphorylation (Carrera *et al.*, 1996) (Fig. 5, lanes 2, 4, 6 and 8 versus lanes 1, 3, 5 and 7). In addition, the tyrosine phosphorylation of proteins of 40–105 kDa was significantly enhanced in a time-dependent manner when sperm samples were incubated in 0.3% BSA-BWW media containing no added Ca^{2+} (Fig. 5, lanes 3, 5 and 7). Pre-incubation with the anti-hGC-G IgG or the control IgG had no effect on the profiles of BSA-induced tyrosine phosphorylation of proteins in the absence of Ca^{2+} (Fig. 5, lanes 9 or 10 versus lane 5) or in the presence of Ca^{2+} (data no shown). As well, human sperm motility was not affected by incubation with the anti-hGC-G IgG (data not shown). Together, our data suggest that hGC-G may not be involved in human sperm capacitation.

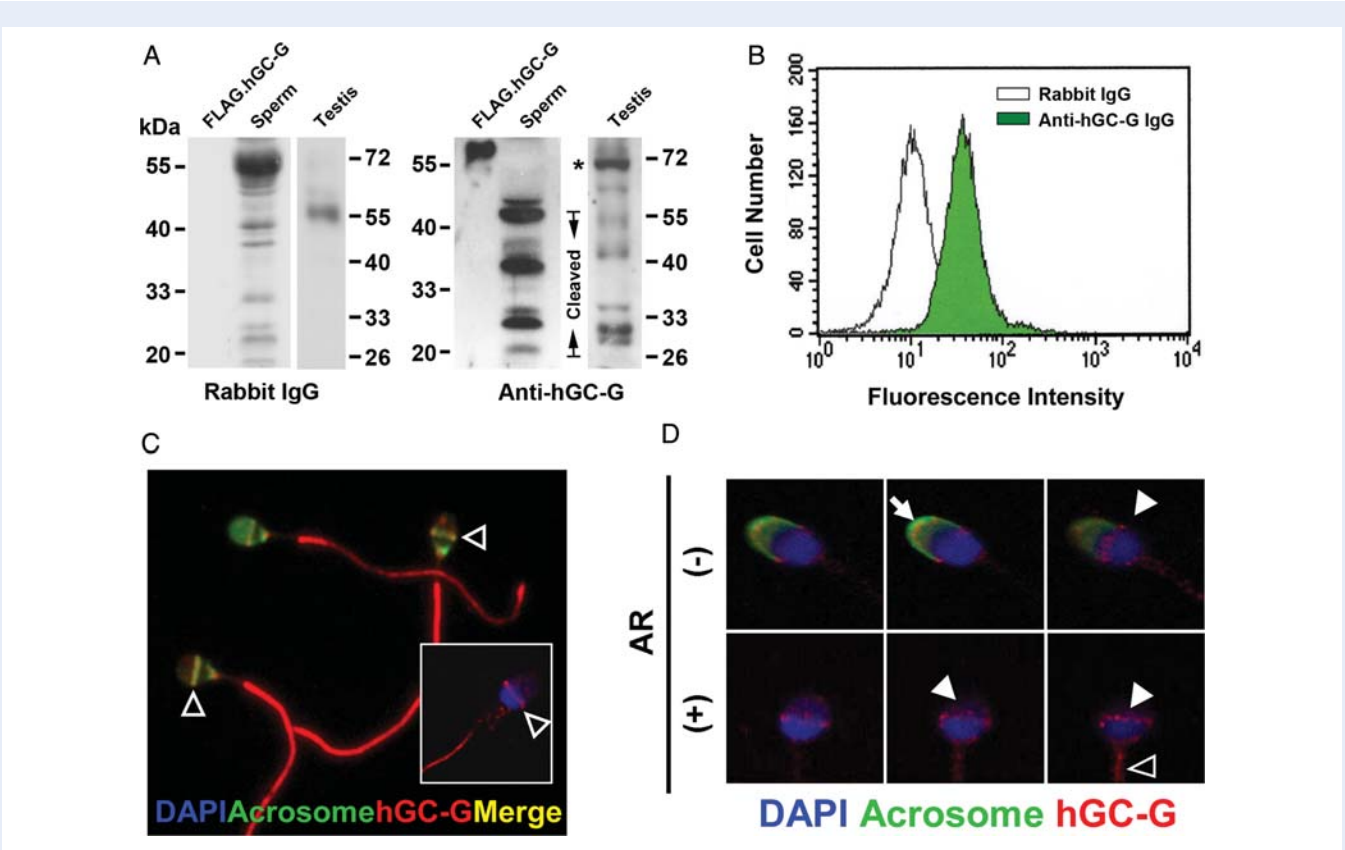

Figure 4 Protein expression and localization of hGC-G in human testis and sperm.

(**A**) Western blot analysis of hGC-G expression in human testis and sperm. Percoll-purified human sperm extracts or testis lysate were separated on SDS-PAGE, electron-blotted and probed with anti-hGC-G IgG. As compared with rabbit IgG, the anti-hGC-G IgG specifically recognized a ~70 kDa precursor protein (asterisk) in the testis and several proteolytic products (30–50 kDa) in human sperm (cleaved). FLAG-hGC-G recombinant protein was used as a control to confirm the antibody specificity. Molecular masses are indicated in kDa. (**B**) Sperm surface expression of hGC-G by flow cytometry analysis. Mature sperm were collected and stained with anti-hGC-G IgG (10 μg/ml) or control rabbit IgG, then FITC-conjugated anti-rabbit IgG secondary antibody, and were analyzed by FACS. (**C**) Light microscopy localization of hGC-G. The photograph shown is a merged image of acrosome (FITC, in green), nucleus (DAPI, in blue), and hGC-G (in red) localization by immunofluorescence on paraformaldehyde-fixed cells. Note the intense labeling on the anterior, equatorial-segment portion of the head and tail of all cells. Magnification: ×400. (**D**) Immunolocalization of hGC-G to the tail and acrosome cap and equatorial segment of head in human sperm. Confocal immunofluroscence images are from paraformaldehyde fixation, with and/or without acrosome-reacted human sperm stained with the anti-hGC-G IgG (in red). The figure shows the merged confocal fluorescence images of anti-hGC-G antibody (in red) and DAPI staining (in blue). Intense immunofluroscence is highly associated with the tail (open arrowhead), acrosome cap (acrosome-intact cells [AR(−)], closed arrow), and equatorial segment of AR-reacted human sperm ([AR(+)], closed arrowheads). The images represent different focal planes of sperm. Magnification: ×1000.

Effect of hGC-G RGD motif on sperm–oocyte recognition

In comparing amino acid sequences, we found that hGC-G contains an RGD motif located in exon 4 of the ECD domain (Supplementary Fig. 1). The RGD motif present in extracellular matrix proteins or membrane-anchored proteins is known to specifically bind with integrin complexes. To examine the binding ability of hGC-G to integrins, we used HEK-293T (integrin expression)-FN (RGD-motif containing) cell binding as a cell platform to test the competition ability of the hGC-G-RGD peptide (12 amino acids long, Table I) on HEK-293T cell binding to the FN-coated culture plate. As shown in Fig. 6A, the cell adhesion percentage of 293T cells on the FN-coated culture plate was much higher than that of the uncoated group ($^{**}P < 0.001$). The addition of the hGC-G RGD peptide significantly suppressed the binding of the HEK-293T cells on the FN-coated culture plate in a dose-dependent manner ($^{*}P < 0.05$, $^{**}P < 0.001$), whereas the non-adhesive mutated hGC-G RGE peptide (12 amino acids long, Table I) had no effect on the cell–matrix binding and thus served as a control (Fig. 6A).

Integrin is known to be expressed on the ooplasm of oocytes (Nixon *et al*., 2007). Given that hGC-G contains an RGD motif and is located at the acrosome cap and equatorial segment of sperm, we then detected whether the hGC-G RGD motif mediated the recognition of human sperm and oocytes. Zona pellucida-free hamster oocytes were pre-incubated with hGC-G RGD or hGC-G RGE peptide at 37°C for 2 h, and then co-incubated with activated human sperm at 37°C for 0–60 min. We analyzed the adhesive sperm number on hamster zona pellucida-free oocytes. As shown in Fig. 6B, as compared with the hGC-G RGE peptide pre-incubation, hGC-G RGD peptide pre-incubation significantly suppressed the binding of human sperm on the zona pellucida-free hamster oocyte ($^{**}P < 0.001$). These results suggest the potential role of the hGC-G-RGD-containing motif in mediating sperm–oocyte recognition.

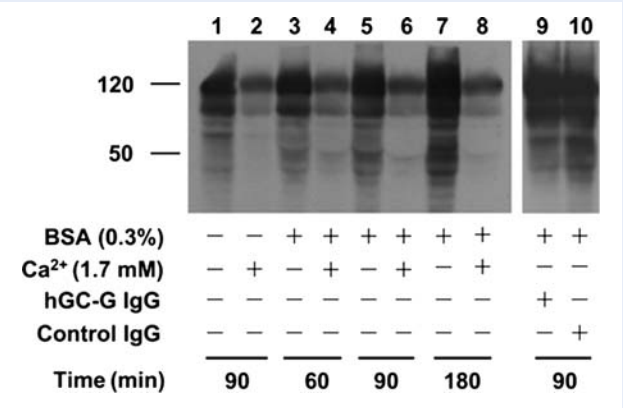

Figure 5 Effect of anti-hGC-G IgG on the bovine serum albumin (BSA)-induced elevation of protein tyrosine phosphorylation in human sperm.

Percoll-purified human sperm were incubated in Ca^{2+}-depriving or Ca^{2+}-containing BWW medium alone for 60–180 min; or were pre-treated with the supplemented anti-hGC-G IgG (20 μM) or control IgG (20 μM) in Ca^{2+}-depriving BWW medium for 15 min, and then incubated with BSA for 90 min (0.3% in a final concentration supplemented with rabbit IgG or anti-hGC-G IgG) to induce protein tyrosine phosphorylation (see 'Materials and Methods'). Relative protein tyrosine phosphorylation in human sperm samples was measured by western blot analysis with anti-phosphotyrosine antibody. Molecular masses are indicated in kDa.

Table 1 Peptides used in this study

hGC-G RGD	RKG**RGD**EGFWKQ*
hGC-G RGE	RKG**RGE**EGFWKQ

*, within exon 4.

Discussion

In this study, we demonstrated that hGC-G is a human sperm cell-surface receptor-like polypeptide and uncovered its role in sperm–oocyte interaction, the critical and complex molecular event for successful fertilization. Recent research in conjunction with genomic and proteomic techniques has uncovered a number of putative cell-surface molecules that regulate the sperm–oocyte interaction; however, the recognition molecules have still remained unclear.

GC-G is the most recent member of the receptor GC family to be identified (Schulz *et al*., 1998; Kuhn *et al*., 2004). The full-length cDNA for mGC-G (*Gucy2g*) was recently identified and originally isolated from the testis (Kuhn *et al*., 2004). The biological function of the mGC-G protein is sperm activation (Huang *et al*., 2006) and early signaling in response to ischemia–reperfusion (I/R)-induced acute renal injury (Lin *et al*., 2008). However, in comparison with the role of GC-G in the mouse model, that in the human orthologue hGC-G was unclear.

To further define the possible biological function of hGC-G, we identified the apparent homologue of GC-G in humans by a comparative genomic approach. Similar to mGC-G mRNA, hGC-G mRNA was selectively and highly expressed in human testis. In addition, in comparison to the mouse orthologue, hGC-G showed high similarity in a conserved allelic gene sequence but with some deletions in the ECD, the cyclase catalytic domain, as well as in-frame termination codons in the deduced coding sequence of cytosolic kinase-like domain. Because of defects in the deduced coding sequence of the kinase-like and cyclase domain, which respond with cGMP-mediated signaling, hGC-G was tentatively suggested to be a non-functional protein (Kuhn, 2009).

In our experiments, we found that although hGC-G contains some defects in gene sequence, it is still expressed as a receptor-like protein in structure. Further experiments by western blot analysis with a specific antibody showed that the hGC-G protein is expressed in ejaculated human sperm. In addition, use of immunocytochemical staining in combination with flow cytometry, epifluorescence and confocal imaging revealed that hGC-G is localized both on the acrosomal cap and equatorial segment of the human sperm head. The equatorial segment protein of sperm head is important for successful fertilization (Wolkowicz *et al*., 2008). Many sperm equatorial-segment proteins have been reported to mediate the sperm–oocyte interaction; examples are: mouse SLLP1 (mouse sperm lysozyme-like protein), located in the equatorial segment of mouse and human spermatozoa (Herrero *et al*., 2005); oxidoreductase ERp57 (Pdi3a, localized on the plasma membrane overlaying the equatorial segment of mouse sperm) (Ellerman *et al*., 2006); and Izumo (a novel member of the immunoglobulin superfamily located on the inner acrosomal membrane and equatorial segment of mouse sperm) (Inoue *et al*., 2005). Thus, the strategic localization of hGC-G on the sperm acrosomal membrane and equatorial segment strongly implies its role in sperm–oocyte interaction.

Furthermore, we found that an RGD-containing motif is present in the coding sequence within the hGC-G ECD domain. The RGD-containing motif is known to interact with integrin to promote cell–cell or cell–extracellular matrix interactions (Huveneers *et al*., 2007). In the sperm–oocyte interaction, the RGD-containing motif of sperm cell-surface proteins has been hypothesized to serve as a recognition site for oocyte binding. Pre-incubation of RGD peptides with oocytes inhibits the sperm–oocyte interaction in the hamster or bovine (Bronson and Fusi, 1990; Shrimali and Reddy, 2000; Eto *et al*., 2002). For example, the ADAM family of sperm cell-surface proteins, such as fertilin α/β (ADAM1/2) and cyritestin (ADAM3), provide the RGD motif to bind integrin α6β1 on oocytes to promote successful fusion (Primakoff and Myles, 2000). However, fertilin β-null sperm still showed ~50% of the successful sperm–oocyte fusion rate, and cyritestin-null sperm showed 100% of the wild-type rate. Furthermore, double knockout of fertilin β and cyritestin in mice showed fusion at ~50% of the wild-type rate (Cho *et al*., 1998; Nishimura *et al*., 2001). In addition, recent reports of $CD46^{-/-}$ (Inoue *et al*., 2003) as well as $CRISP1^{-/-}$ (Da Ros *et al*., 2008) also showed no difference in fertility as compared with the control group. These results strongly suggest that the potential candidate gene for sperm–oocyte interaction still requires further validation by a gene targeting approach. Together, multiple cooperation systems must exist in the sperm–oocyte interaction to facilitate gamete fusion efficiency in physiology.

In our experiments, hGC-G seemed not to be involved in capacitation-associated protein tyrosine phosphorylation of human spermatozoa. However, pre-incubation of hGC-G-RGD peptide

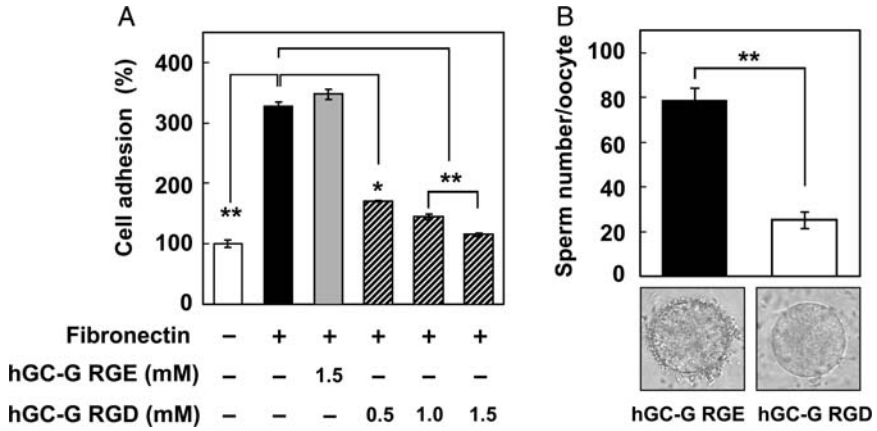

Figure 6 Effect of hGC-G RGD motif in sperm–oocyte interaction.

(**A**) The binding ability of hGC-G-RGD to integrin. The competition ability of hGC-G-RGD or hGC-G-RGE peptide on the interaction of 293T cells (with integrin) to fibronectin (FN, 10 μg/ml) is shown. The cell adhesion percentage of 293T cells on the FN-coated culture plate is much higher than that without FN-coated (**denotes that the difference in cell adhesion percentage on the FN-coated plate is significant at $P < 0.001$). The inhibition effect of hGC-G RGD peptide (0, 0.5, 1.0 and 1.5 mM) or hGC-G-RGE (1.5 mM) on the cell adhesion percentage of 293T cells on the FN-coated culture plate was examined (*$P < 0.05$, **$P < 0.001$). (**B**) Effect of hGC-G RGD peptide or hGC-G RGE (0.5 mM) on adhesion of sperm and zona pellucida-free oocytes. **denotes that the difference from the hGC-G RGE pretreatment is significant at $P < 0.001$. Represents mean ± SD of at least three independent determinations for each condition.

with hamster oocytes significantly reduced the binding ability of human spermatozoa on zona pellucida-free hamster oocytes. Together, our data suggest that the equatorial-segment protein hGC-G may play a role in sperm–oocyte interaction through its RGD motif. Of note, we tested, but did not observe an inhibitory effect of anit-hGC-G IgG on sperm adhesion to oocytes. These results may be due to this antibody being raised by a peptide immunogen distinct from the RGD motif site, therefore not targeting the non-RGD site. However, we cannot formally exclude that the RGD peptide may target other sperm protein(s) other than hGC-G. Regardless, further studies producing additional specific anti-hGC-G antibodies against the adhesive RGD motif are important to clarify this issue.

Within the GC gene family, hGC-D, like hGC-G, was proposed to be a pseudogene in humans by genomic prediction (Potter, 2005). However, unlike the hGC-G gene, which still codes for a receptor-like product containing the ECD, transmembrane domain, and partial kinase domain, the hGC-D gene contains large deletions of exons 2/4/5, which almost remove the ECD and transmembrane domain. In addition, deletion of exons 4/5 leads to a frame shift and truncates the protein before the kinase and catalytic domains. Thus, the GC-D gene was suggested to be degenerated during primate evolution (Young *et al*., 2007).

In this respect, in terms of gene and protein level, we have demonstrated hGC-G expression by a genomic approach, mRNA/protein detection and cellular localization. In protein expression, western blot analysis revealed a proteolytic process of hGC-G similar to mGC-G during sperm maturation (Fig. 4A, testis panel). A similar proteolytic modification of fertilin α/β also plays important roles in sperm–oocyte recognition (Blobel *et al*., 1990). The proteolytic processing of fertilin, and perhaps other sperm proteins, has been suggested to trigger the relocalization of fertilin from the whole sperm head to the posterior head to expose an epitope for sperm–oocyte interactions (Blobel, 2000). Likewise, an hGC-G fragment anchored on the sperm surface may use a similar proteolytic processing to expose its RGD-containing motif and exert its biological function in the sperm–oocyte interaction.

In summary, we demonstrated that the hGC-G is a cell-surface protein expressed on the acrosomal and equatorial segment of human sperm, and this novel GC receptor may participate in sperm–oocyte interaction through its RGD-containing motif. Functional study of the proposed pseudogene hGC-G could shed some light on the possible biological function of this pseudogene family identified by genomic research.

Supplementary data

Supplementary data are available at http://humrep.oxfordjournals.org/.

Funding

This research was supported by the National Science Council, Taiwan (NSC 97-2320-B-001-009-MY3 to R.B.Y. and NSC95-2311-B-038-002-MY2, NSC97-3111-B-038-001 to Y.H.H.) and Taipei Medical University and Hospital (96TMU-TMUH-12).

References

Anderson DJ, Abbott AF, Jack RM. The role of complement component C3b and its receptors in sperm–oocyte interaction. *Proc Natl Acad Sci USA* 1993;**90**:10051–10055.

Biggers JD, Whitten WK, Whittingham DG. The culture of mouse embryos *in vitro*. In Daniel JD (ed). *Methods in Mammalian Embryology*. San Francisco: Freeman, 1971, 86–116.

Bigler D, Takahashi Y, Chen MS, Almeida EA, Osbourne L, White JM. Sequence-specific interaction between the disintegrin domain of mouse ADAM 2 (fertilin β) and murine eggs. Role of the α6 integrin subunit. *J Biol Chem* 2000;**275**:11576–11584.

Blobel CP. Functional processing of fertilin: evidence for a critical role of proteolysis in sperm maturation and activation. *Rev Reprod* 2000; **5**:75–83.

Blobel CP, Myles DG, Primakoff P, White JM. Proteolytic processing of a protein involved in sperm-egg fusion correlates with acquisition of fertilization competence. *J Cell Biol* 1990;**111**:69–78.

Brandelli A, Miranda PV, Tezon JG. Participation of glycosylated residues in the human sperm acrosome reaction. Possible role of N-acetylglucosaminidase. *Biochim Biophys Acta* 1994;**1220**:299–304.

Bronson RA, Fusi F. Evidence that an Arg-Gly-Asp adhesion sequence plays a role in mammalian fertilization. *Biol Reprod* 1990; **43**:1019–1025.

Carrera A, Moos J, Ning XP, Gerton GL, Tesarik J, Kopf GS, Moss SB. Regulation of protein tyrosine phosphorylation in human sperm by a calcium/calmodulin-dependent mechanism: identification of A kinase anchor proteins as major substrates for tyrosine phosphorylation. *Dev Biol* 1996;**180**:284–296.

Chinkers M, Garbers DL, Chang MS, Lowe DG, Chin HM, Goeddel DV, Schulz S. A membrane form of guanylate cyclase is an atrial natriuretic peptide receptor. *Nature* 1989;**338**:78–83.

Cho C, Bunch DO, Faure JE, Goulding EH, Eddy EM, Primakoff P, Myles DG. Fertilization defects in sperm from mice lacking fertilin beta. *Science* 1998;**281**:1857–1859.

Cuasnicu PS, Gonzalez Echeverria F, Piazza AD, Cameo MS, Blaquier JA. Antibodies against epididymal glycoproteins block fertilizing ability in rat. *J Reprod Fertil* 1984;**72**:467–471.

Da Ros VG, Maldera JA, Willis WD, Cohen DJ, Goulding EH, Gelman DM, Rubinstein M, Eddy EM, Cuasnicu PS. Impaired sperm fertilizing ability in mice lacking Cysteine-RIch Secretory Protein 1 (CRISP1). *Dev Biol* 2008; **320**:12–18.

Ellerman DA, Myles DG, Primakoff P. A role for sperm surface protein disulfide isomerase activity in gamete fusion: evidence for the participation of ERp57. *Dev Cell* 2006;**10**:831–837.

Eto K, Huet C, Tarui T, Kupriyanov S, Liu HZ, Puzon-McLaughlin W, Zhang XP, Sheppard D, Engvall E, Takada Y. Functional classification of ADAMs based on a conserved motif for binding to integrin alpha 9 beta 1: implications for sperm-egg binding and other cell interactions. *J Biol Chem* 2002;**277**:17804–17810.

Evans JP. The molecular basis of sperm–oocyte membrane interactions during mammalian fertilization. *Hum Reprod Update* 2002;**8**:297–311.

Evans JP, Schultz RM, Kopf GS. Mouse sperm-egg plasma membrane interactions: analysis of roles of egg integrins and the mouse sperm homologue of PH-30 (fertilin) beta. *J Cell Sci* 1995;**108**:3267–3278.

Fulle HJ, Vassar R, Foster DC, Yang RB, Axel R, Garbers DL. A receptor guanylyl cyclase expressed specifically in olfactory sensory neurons. *Proc Natl Acad Sci USA* 1995;**92**:3571–3575.

Garbers DL. The guanylyl cyclase receptors. *Methods* 1999;**19**:477–484.

Herrero MB, Mandal A, Digilio LC, Coonrod SA, Maier B, Herr JC. Mouse SLLP1, a sperm lysozyme-like protein involved in sperm-egg binding and fertilization. *Dev Biol* 2005;**284**:126–142.

Huang YH, Wei CC, Su YH, Wu BT, Ciou YY, Tu CF, Cooper TG, Yeung CH, Chu ST, Tsai MT *et al*. Localization and characterization of an orphan receptor, guanylyl cyclase-G, in mouse testis and sperm. *Endocrinology* 2006;**147**:4792–4800.

Huveneers S, Truong H, Danen HJ. Integrins: signaling, disease, and therapy. *Int J Rad Biol* 2007;**83**:743–751.

Inoue N, Ikawa M, Nakanishi T, Matsumoto M, Nomura M, Seya T, Okabe M. Disruption of mouse CD46 causes an accelerated spontaneous acrosome reaction in sperm. *Mol Cell Biol* 2003; **23**:2614–2622.

Inoue N, Ikawa M, Isotani A, Okabe M. The immunoglobulin superfamily protein Izumo is required for sperm to fuse with eggs. *Nature* 2005; **434**:234–238.

Koller KJ, Lowe DG, Bennett GL, Minamino N, Kangawa K, Matsuo H, Goeddel DV. Selective activation of the B natriuretic peptide receptor by C-type natriuretic peptide (CNP). *Science* 1991;**252**:120–123.

Kuhn M. Function and Dysfunction of Mammalian Membrane Guanylyl Cyclase Receptors: Lessons from Genetic Mouse Models and Implications for Human Diseases. Handb Exp Pharmacol: cGMP: Generators, Effectors and Therapeutic Implications, **Vol. 191**. Berlin Heidelberg: Springer, 2009, 47–69.

Kuhn M, Ng CK, Su YH, Kilić A, Mitko D, Bien-Ly N, Kömüves LG, Yang RB. Identification of an orphan guanylate cyclase receptor selectively expressed in mouse testis. *Biochem J* 2004;**379**:385–393.

Lin H, Cheng CF, Hou HH, Lian WS, Chao YC, Ciou YY, Djoko B, Tsai MT, Cheng CJ, Yang RB. Disruption of guanylyl cyclase-G protects against acute renal injury. *J Am Soc Nephrol* 2008;**19**:339–348.

Lowe DG, Chang MS, Hellmiss R, Chen E, Singh S, Garbers DL, Goeddel DV. Human atrial natriuretic peptide receptor defines a new paradigm for second messenger signal transduction. *EMBO J* 1989; **8**:1377–1384.

Lowe DG, Dizhoor AM, Liu K, Gu Q, Spencer M, Laura R, Lu L, Hurley JB. Cloning and expression of a second photoreceptor-specific membrane retina guanylyl cyclase (RetGC), RetGC-2. *Proc Natl Acad Sci USA* 1995;**92**:5535–5539.

Matsuoka I, Mori T, Sato T, Sakai M, Kurihara K. Identification of novel guanylyl cyclases from chemosensory tissues of rat and cattle. *Biochem Biophys Res Commun* 1995;**216**:242–248.

McNicoll N, Gagnon J, Rondeau JJ, Ong H, De Léan A. Localization by photoaffinity labeling of natriuretic peptide receptor-A binding domain. *Biochemistry* 1996;**35**:12950–12956.

Nicolson G, Yanagimachi H, Yanagimachi R. Ultrastructural localization of lectin-binding sites on the zonae pellucidae and plasma membrane of mammalian egg. *J Cell Biol* 1975;**66**:263–273.

Nishimura H, Cho C, Branciforte DR, Myles DG, Primakoff P. Analysis of loss of adhesive function in sperm lacking cyritestin or fertilin β. *Dev Biol* 2001;**233**:204–213.

Nixon B, Aitken RJ, McLaughlin EA. New insights into the molecular mechanisms of sperm-egg interaction. *Cell Mol Life Sci* 2007; **64**:1805–1823.

Potter LR. Domain analysis of human transmembrane guanylyl cyclase receptors: implications for regulation. *Front Biosci* 2005;**1**:1205–1220.

Primakoff P, Myles DG. The ADAM gene family: surface proteins with adhesion and protease activity. *Trends Genet* 2000;**16**:83–87.

Schlossmann J, Feil R, Hofmann F. Signaling through NO and cGMP-dependent protein kinases. *Ann Med* 2003;**35**:21–27.

Schulz S, Singh S, Bellet RA, Singh G, Tubb DJ, Chin H, Garbers DL. The primary structure of a plasma membrane guanylate cyclase demonstrates diversity within this new receptor family. *Cell* 1989; **58**:1155–1162.

Schulz S, Green CK, Yuen PS, Garbers DL. Guanylyl cyclase is a heat-stable enterotoxin receptor. *Cell* 1990;**63**:941–948.

Schulz S, Wedel BJ, Matthews A, Garbers DL. The cloning and expression of a new guanylyl cyclase orphan receptor. *J Biol Chem* 1998; **273**:1032–1037.

Shrimali RK, Reddy KV. Integrins and disintegrins: the candidate molecular players in sperm-egg interaction. *Indian J Exp Biol* 2000;**38**:415–424.

Shyjan AW, de Sauvage FJ, Gillett NA, Goeddel DV, Lowe DG. Molecular cloning of a retina-specific membrane guanylyl cyclase. *Neuron* 1992; **9**:727–737.

Takahashi Y, Bigler D, Ito Y, White JM. Sequence-specific interaction between the disintegrin domain of mouse ADAM 3 and murine eggs: role of β1 integrin-associated proteins CD9, CD81, and CD98. *Mol Biol Cell* 2001;**12**:809–820.

Tamura N, Chrisman TD, Garbers DL. The regulation and physiological roles of the guanylyl cyclase receptors. *Endocr J* 2001;**48**:611–634.

Thompson DK, Garbers DL. Dominant negative mutations of the guanylyl cyclase-A receptor. Extracellular domain deletion and catalytic domain point mutations. *J Biol Chem* 1995;**270**:425–430.

Vaandrager AB, De Jonge HR. Effect of cyclic GMP on intestinal transport. *Adv Pharmacol* 1994;**26**:253–283.

van den Akker F, Zhang X, Miyagi M, Huo X, Misono KS, Yee VC. Structure of the dimerized hormone-binding domain of a guanylyl-cyclase-coupled receptor. *Nature* 2000;**406**:101–104.

Visconti PE, Bailey JL, Moore GD, Pan D, Olds-Clarke P, Kopf GS. Capacitation of mouse spermatozoa. I. Correlation between the capacitation state and protein tyrosine phosphorylation. *Development* 1995;**121**:1129–1137.

Warner TD, Mitchell JA, Sheng H, Murad F. Effects of cyclic GMP on smooth muscle relaxation. *Adv Pharmacol* 1994;**26**:171–194.

Wolkowicz MJ, Digilio L, Klotz K, Shetty J, Flickinger CJ, Herr JC. Equatorial segment protein (ESP) is a human alloantigen involved in sperm-egg binding and fusion. *J Androl* 2008;**29**:272–282.

Young JM, Waters H, Dong C, Fulle HJ, Liman ER. Degeneration of the olfactory guanylyl cyclase D gene during primate evolution. *PLoS ONE* 2007;**2**:e884.

Yuan R, Primakoff P, Myles DG. A role for the disintegrin domain of cyritestin, a sperm surface protein belonging to the ADAM family, in mouse sperm-egg plasma membrane adhesion and fusion. *J Cell Biol* 1997;**137**:105–112.

Zarelli VE, Ruete MC, Roggero CM, Mayorga LS, Tomes CN. PTP1B dephosphorylates N-ethylmaleimide-sensitive factor and elicits SNARE complex disassembly during human sperm exocytosis. *J Biol Chem* 2009;**284**:10491–11503.

Submitted on April 28, 2009; resubmitted on August 11, 2009; accepted on September 10, 2009